

Azimuthal vortex clusters in Bose-Einstein condensatesVolodymyr M. Lashkin,¹ Anton S. Desyatnikov,² Elena A. Ostrovskaya,^{2,*} and Yuri S. Kivshar²¹*Institute for Nuclear Research, Pr. Nauki 47, Kiev 03680, Ukraine*²*Nonlinear Physics Centre, Research School of Physics and Engineering, The Australian National University, Canberra, ACT 0200, Australia*

(Received 27 November 2011; published 17 January 2012)

We describe, analytically and numerically, topologically nontrivial stationary states with azimuthal modulation of density in a repulsive Bose-Einstein condensate (BEC) confined in a harmonic trap. We show that, depending on the number of density peaks and total topological charge, these states can have a sophisticated phase texture associated with a vortex cluster. For a given topological charge, the form of density distribution and the structure of phase singularities are uniquely linked, thus simultaneous phase and density modulation enforces the formation of a vortex cluster both in rotating and in nonrotating BEC clouds.

DOI: [10.1103/PhysRevA.85.013620](https://doi.org/10.1103/PhysRevA.85.013620)

PACS number(s): 03.75.Lm

I. INTRODUCTION

The topologically nontrivial collective excitations of Bose-Einstein condensates (BECs) containing quantized currents (vortices) are one of the most intensely studied phenomena in the physics of ultracold atomic gases. The hierarchy of such states has been thoroughly investigated both theoretically and experimentally. It includes a single vortex line in a harmonically confined rotating BEC [1–5]; a vortex cluster, e.g., a vortex-antivortex dipole [1,5,6], a tripole [7,8], or a quadrupole [1], in both rotating and nonrotating [7,9] BEC clouds. On top of this hierarchy are hexagonal (Abrikosov) vortex lattices forming as a robust steady state in rotating clouds [10,11] or transient honeycomb lattices forming via interference of fragmented nonrotating BECs [12–14]. In contrast to the Kibble-Zurek mechanism of spontaneous vortex production during the rapid temperature quench through the BEC transition [15,16], the route that enables one to move, in a controlled manner, from one to many vortices in a (near-)zero-temperature BEC cloud is the rotation of the BEC cloud [17–20]. The number of vortices entering the condensate above a certain critical velocity of rotation increases with growing velocity, until, for a sufficiently large number of vortices, a stationary Abrikosov lattice supported by repulsive intervortex interactions is formed [10].

Recently, a novel topological state—the *azimuthon vortex*—was predicted to exist in BECs with a negative scattering length in both single- [21] and two-component [22] condensates. These states were first described theoretically [23–25] and observed experimentally [26] in the context of optical singular beams in nonlinear media with a focusing nonlinearity. The existence of optical azimuthons was also predicted in azimuthally modulated Bessel lattices induced in a defocusing Kerr medium [27]. A basic azimuthon is a spatially localized vortex of a single or multiple topological charge (i.e., phase winding number around the vortex core) and *azimuthal density modulation* [21,23], so that the spatial density profile displays multiple peaks. As such, an azimuthon represents a natural link between a single vortex with quantized circulation and a cluster of solitons [28,29] (with or without a total angular

momentum). The quirky feature of azimuthons emphasized in [23] is that, due to the azimuthal modulation of energy flow, for the same topological charge and number of peaks, they can display *positive, negative, or zero angular velocity*.

Here we describe *azimuthal vortex clusters*: higher-order multipeaked BEC azimuthons that contain multiple phase singularities. We construct an analytical theory of such stationary states both for a noninteracting BEC and for an interacting (nonlinear) BEC with a positive scattering length confined in an axisymmetric potential. Our theory comprehensively links the nonlinear azimuthons with the linear modes of a BEC in the confining trap (the existence of such a link between nonlinear and linear states was hinted at in the recent study of optical azimuthons in weakly nonlinear waveguides [30]). Using our theory, we demonstrate, both analytically and numerically, that a density-modulated vortex of a certain topological charge gives rise to an azimuthal cluster of single-charged vortices arranged in a strictly deterministic manner. In some ways, this mechanism is analogous to the formation of gap BEC vortices in optical lattices [31] and optical multivortex solitons in photonic lattices [32–34]; there, the density modulation enforced by the symmetry of the lattice potential enforces the symmetry of the phase texture. Excitation of a specific azimuthal cluster in a BEC therefore provides a route for controlled generation of multiple-vortex states of different symmetries both *with* and *without* collective rotation of the BEC cloud. Ultimately, azimuthal vortex clusters provide a smooth transition from a single-vortex state to vortex lattices with a large number of singularities and provide an additional means of phase texture control in nonrotating BECs [35].

II. MODEL

We model a BEC confined in an axisymmetric “pancake” trap, i.e., we assume a weak harmonic confinement in (x, y) dimensions and tight confinement in the transverse z dimension, with the respective trapping frequencies Ω and Ω_z , with $\Omega_z \gg \Omega$. Assuming that the energy of the mean-field interaction is much lower than the characteristic energy of the transverse confinement, the condensate wave function is separable into the transverse, i.e., z dependent, and radial parts [36], and the mean-field model takes an effectively two-dimensional (2D) form. The dynamics of the condensate

*ost124@physics.anu.edu.au

is then described by the normalized Gross-Pitaevskii equation (GPE) for the radial wave function $\psi(x, y)$,

$$i \frac{\partial \psi}{\partial t} = -\nabla_{\perp}^2 \psi + (x^2 + y^2)\psi + \sigma |\psi|^2 \psi, \quad (1)$$

where $\nabla_{\perp}^2 = \partial^2/\partial x^2 + \partial^2/\partial y^2$. Here time is measured in units of $2/\Omega_z$, length in units of $a_0 = \sqrt{\hbar/(m\Omega_z)}$, with m being the atomic mass, and the wave function in units of $a_0^{-3/2}$. The (dimensionless) wave function in the transverse z dimension is assumed to be that of a ground state of the quantum harmonic oscillator normalized to 1. The radial component of the wave function is scaled as $\psi(x, y) \rightarrow \sqrt{g_{2D}}\psi(x, y)$, where $g_{2D} = 4\sqrt{2\pi}(|a|/a_0)\lambda$ are proportional to the scattering lengths, a , and $\lambda = \Omega/\Omega_z \ll 1$. For the typical aspect ratios of the 2D trapping achieved in the experiment, $\lambda \sim 10^{-1}-10^{-2}$ [37,38]. The only remaining parameter in Eq. (1) is the sign of the scattering length, σ . In what follows, we consider both noninteracting ($\sigma = 0$) and nonlinear BEC ($\sigma \neq 0$), paying particular attention to the case of the positive scattering length, i.e., repulsive interatomic interactions, $\sigma = +1$.

Equation (1) conserves the norm of the radial wave function (the normalized number of particles),

$$\mathcal{N} = \int |\psi|^2 dx dy; \quad (2)$$

the z component of the angular momentum,

$$\mathcal{M}_z = \text{Im} \int [\psi^*(\mathbf{r} \times \nabla_{\perp} \psi)]_z dx dy; \quad (3)$$

and the total energy (Hamiltonian),

$$\mathcal{E} = \int \left\{ |\nabla_{\perp} \psi|^2 + (x^2 + y^2)|\psi|^2 + \frac{\sigma}{2} |\psi|^4 \right\} dx dy. \quad (4)$$

We seek solutions of Eq. (1) which are stationary in the frame rotating with the angular velocity ω . In polar coordinates (r, φ) , such solutions of the form

$$\psi(r, \varphi, t) = \Phi(r, \varphi - \omega t) \exp(-i\mu t), \quad (5)$$

where μ is the chemical potential in the rotating frame, satisfy the equation

$$\frac{\partial^2 \Phi}{\partial r^2} + \frac{1}{r} \frac{\partial \Phi}{\partial r} + \frac{1}{r^2} \frac{\partial^2 \Phi}{\partial \theta^2} - i\omega \frac{\partial \Phi}{\partial \theta} - r^2 \Phi - \sigma |\Phi|^2 \Phi = -\mu \Phi, \quad (6)$$

where $\theta = \varphi - \omega t$. In Cartesian coordinates, Eq. (6) becomes

$$\begin{aligned} \nabla_{\perp}^2 \Phi - i\omega \left(x \frac{\partial}{\partial y} - y \frac{\partial}{\partial x} \right) \Phi - [(x^2 + y^2) + \sigma |\Phi|^2] \Phi \\ = -\mu \Phi. \end{aligned} \quad (7)$$

III. STATIONARY STATES OF NONINTERACTING BEC ($\sigma = 0$)

In the linear limit, $\sigma = 0$, Eq. (7) coincides with the Schrödinger equation for an electron wave function in a homogeneous magnetic field. The corresponding eigenfunctions are well known:

$$\mathcal{L}_{n,\pm m}(x, y) = e^{-(x^2+y^2)/2} \left(\frac{x \pm iy}{\sqrt{2}} \right)^m L_n^m(x^2 + y^2), \quad (8)$$

where $L_n^m(\xi)$ is the generalized Laguerre polynomial, and the corresponding eigenvalues are

$$\mu_{n,\pm m} = 4n + 2|m| + 2 \mp m\omega, \quad (9)$$

where n and m are non-negative integers. In what follows we restrict our consideration to the nodeless case $n = 0$, so that the eigenfunctions and eigenvalues are

$$\Phi_{\pm m} = \mathcal{L}_{0,\pm m}(x, y) = e^{-(x^2+y^2)/2} \left(\frac{x \pm iy}{\sqrt{2}} \right)^m \quad (10)$$

and

$$\mu_{\pm m} = 2|m| + 2 \mp m\omega. \quad (11)$$

As can be seen from the structure of Eq. (10), it describes stationary vortex states with the topological charge m , or the ground states $m = 0$, of a noninteracting BEC in a 2D harmonic trap. These stationary solutions of GPE are not valid in the nonlinear case, $\sigma \neq 0$, however, the bifurcation from linear to nonlinear solutions of Eq. (7) is possible above the critical value $\mu > \mu_{\pm m}$, where $\mu_{\pm m}$ is determined by Eq. (11). The corresponding nonlinear ground states and vortices can be found numerically.

Our primary task is to describe nonlinear solutions of Eq. (7) that are different from fundamental ground states and vortices (in the nodeless case, $n = 0$). To this end we first consider the case $\sigma = 0$. It is clear that the only possible candidate for the solution different from Eq. (10) is a superposition of the linear modes $\Phi_{\pm m}$ with equal corresponding eigenvalues μ determined by Eq. (11). It can easily be seen from Eq. (11) that there exists *the only* way to construct such a superposition. It has the form

$$\Phi = c_1 \Phi_{-k} + c_2 \Phi_l, \quad (12)$$

where k and l are positive, the coefficients c_1 and c_2 are arbitrary, and $\mu_{-k} = \mu_l$. This expression yields the only possible (for the fixed k and l) value of ω_{lin} and the eigenvalue μ_{lin} corresponding to the linear mode (12):

$$\omega_{\text{lin}} = \frac{2(l-k)}{l+k}, \quad (13)$$

$$\mu_{\text{lin}} = k(\omega_{\text{lin}} + 2) + 2. \quad (14)$$

If nonlinear states with similar phase and density structure exist, then Eqs. (13) and (14) represent the bifurcation points on the (ω, μ) plane where nonlinear stationary states branch off the linear modes.

IV. STATIONARY STATES OF INTERACTING BEC ($\sigma = 1$)

In the nonlinear case, $\sigma \neq 0$, Eq. (7) is not integrable, and we resort to variational analysis to find approximate stationary states. Stationary solutions of Eq. (6) in the form of (5) resolve the variational problem $\delta S = 0$ for the functional $S = \mathcal{E} - \mu \mathcal{N} - \omega \mathcal{M}_z$. Bearing in mind the structure of the linear stationary state, Eq. (12), we take a trial function in the form of the superposition of two vortices with the topological charges $-k$ and l :

$$\Phi = A e^{-\xi^2/2} (\xi^k e^{-ik\theta} + s \xi^l e^{il\theta}), \quad (15)$$

where $\xi = r/a$, k , and l are positive integers; A , a , and s are unknown parameters to be determined by the variational

procedure. In the limiting cases $s = 0$ and $s \gg 1$, the ansatz models a single vortex with charge $-k$ or l , respectively. Note that a similar ansatz appears in the stability analysis of a vortex soliton of charge $-k$, superimposed with the perturbation mode of charge $m = l + k$ and amplitude s [39]. Instead of a low amplitude $s \ll 1$ in the linear stability analysis, here we cover the whole range of values s , however, the linearization allows for a more general superposition that accounts for modes with both $+m$ and $-m$.

Substituting Eq. (15) into Eqs. (2), (3), and (4), we arrive at the following expression for the functional S :

$$S(A, a, s) = \mathcal{E}_1 + \mathcal{E}_2 + \mathcal{E}_3 - \mu \mathcal{N} - \omega \mathcal{M}_z. \quad (16)$$

The term \mathcal{E}_1 corresponds to the kinetic energy,

$$\begin{aligned} \mathcal{E}_1 = \pi A^2 [2k^2(k-1)! + 2s^2 l^2(l-1)! + (k+1)! \\ + s^2(l+1)! - 2kk! - 2s^2 ll!], \end{aligned} \quad (17)$$

and

$$\mathcal{E}_2 = \pi A^2 a^4 [(k+1)! + s^2(l+1)!] \quad (18)$$

is the energy due to the harmonic trap. The contribution from the nonlinear interaction is

$$\mathcal{E}_3 = \pi A^4 a^2 \left[\frac{(2k)!}{2^{2k+1}} + \frac{s^4(2l)!}{2^{2l+1}} + \frac{s^2(k+l)!}{2^{k+l-1}} \right], \quad (19)$$

the number of particles is

$$\mathcal{N} = \pi A^2 a^2 (k! + s^2 l!), \quad (20)$$

and the angular momentum is

$$\mathcal{M}_z = \pi A^2 a^2 (s^2 ll! - kk!). \quad (21)$$

The parameters A , a , and s are determined from the system of equations $\partial S / \partial A = 0$, $\partial S / \partial a = 0$, and $\partial S / \partial s = 0$.

One can find a set of various solutions satisfying the variational problem. As a general rule, the stationary state has $N = k + l$ peaks and $N + 1$ singularities in the phase, including N singularities with the topological charge $+1$ on the periphery and one singularity with the charge $-k$ at the center, so that the total topological charge is $m = N - k = l$. In addition to μ and the rotational frequency ω , we characterize the stationary states by the two topological charges $k = N - m$ and l and denote the corresponding structure $(-k, l)$ (without loss of generality, we assume $l \geq k$). Existence domains for various $(-k, l)$ azimuthal clusters on the plane (μ, ω) are presented in Fig. 1. The bifurcation points (i.e., tips of the existence domains in Fig. 1) are in perfect agreement with analytical expressions (13) and (14), which can be rewritten in terms of N and m :

$$\omega_{\text{lin}} = \frac{2(2m - N)}{N}, \quad (22)$$

$$\mu_{\text{lin}} = (N - m)(2 + \omega_{\text{lin}}) + 2. \quad (23)$$

Examples of five-peak states [amplitudes, $|\Phi|$, and phases, $\arg(\Phi)$], corresponding to existence domains 4 and 6 in Fig. 1, are shown in Fig. 2. As can be seen, the two states with the same number of peaks differ by the total topological charge, which results in a different structure of singularities. This structure can be viewed as a cluster of *six* individual vortices

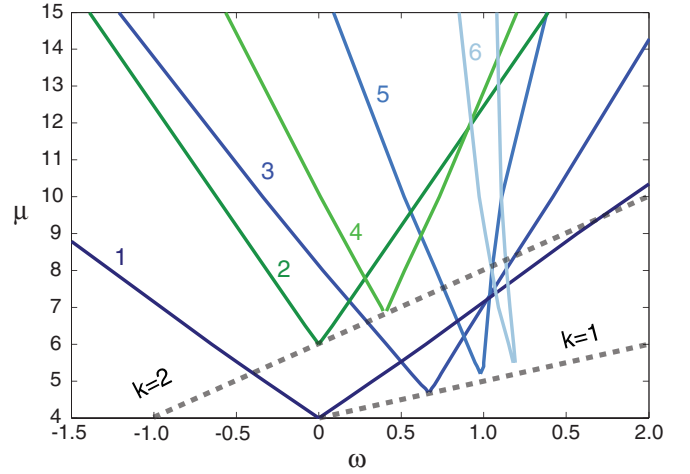


FIG. 1. (Color online) Existence regions for azimuthal clusters $(-k, l)$ with N peaks in the density profile in the parameter space $\{\omega, \mu\}$. Azimuthal clusters exist within the angular sectors bordered from below by the numbered curves. For $k = 1$, existence domains for the two-peak azimuthon $(-1, 1)$ (curve 1; $N = 2$) and clusters $(-1, 2)$ (curve 3; $N = 3$), $(-1, 3)$ (curve 5; $N = 4$), and $(-1, 4)$ (curve 6; $N = 5$) are shown. For $k = 2$, existence domains for clusters $(-2, 2)$ (curve 2; $N = 4$) and $(-2, 3)$ (curve 4; $N = 5$) are shown. Dashed lines show the dependences $\mu_{\text{lin}}(\omega_{\text{lin}})$ in the linear limit ($\sigma = 0$) for $k = 1, 2$.

with positive and negative topological charges. All the single-quantized vortices on the periphery have charge $+1$, however, the central vortex in the cluster has charge $-k = m - N$, which is determined by both the total topological charge and the density modulation.

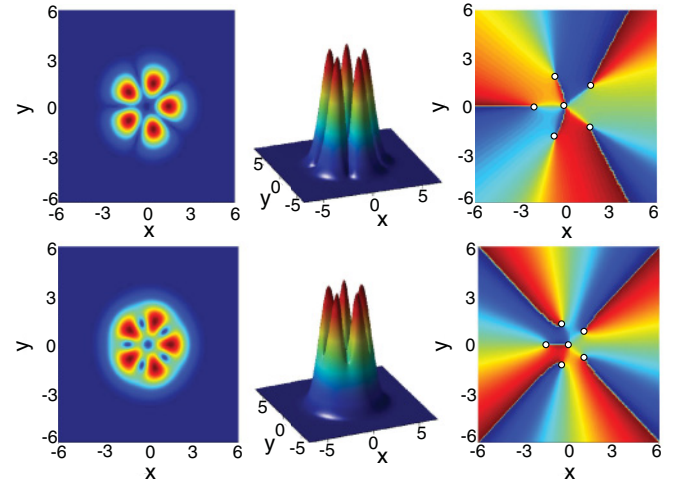


FIG. 2. (Color online) Amplitude, $|\Phi|$, and phase structure of stationary five-peak clusters from the existence domains in Fig. 1) bordered by curves 5 (top row) and 6 (bottom row). Top row: five-peak cluster $(-2, 3)$ ($\mu = 10$, $\omega = 0.45$) containing six singularities: five on the periphery, with charge $+1$, and one at the center, with charge -2 . The total charge is $m = l = 3$. Bottom row: five-peak azimuthal cluster $(-1, 4)$ ($\mu = 7$, $\omega = 1.12$) containing six singularities: five on the periphery, with charge $+1$, and one singularity at the center, with charge -1 . The total charge is $m = l = 4$. The phase changes from 0 (blue) to 2π (red); vortex positions are shown by circles.

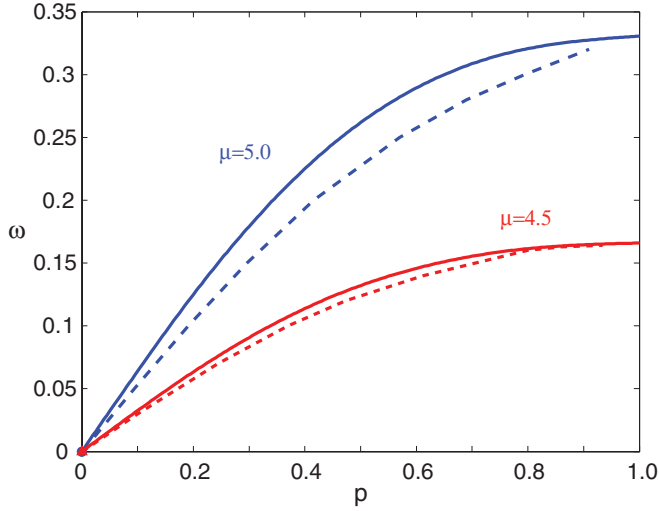


FIG. 3. (Color online) Dependence of the angular velocity ω of the two-peak azimuthally modulated single-charge vortex (azimuthon) $\langle -1, 1 \rangle$ on the modulational depth p for two values of μ . Results of the variational analysis (solid lines) and numerical solution of the model equation (dashed lines) are presented.

The variational ansatz, when used as an initial guess, allows us to find exact numerical solutions of Eq. (7) by a method similar to the one described in [21], with a high accuracy [40]. To quantify the agreement between the variational and the numerical solutions, we consider azimuthal clusters with $k = l$ (i.e., $N = 2m$) and introduce the modulation depth parameter in the following way: $p = (s - 1)/(s + 1)$. This parameter defines azimuthal (θ) modulation in the variational ansatz previously introduced for azimuthons (see, e.g., [21]), $\Phi(\theta) \sim \cos m\theta + ip \sin m\theta$, and can be extracted directly from the numerical results $p = \max |\text{Im } \Phi| / \max |\text{Re } \Phi|$. For a given cluster $\langle -k, l \rangle$ within the existence domain (Fig. 1), the depth of the density modulation quantifies the extent to which the internal flow of particles within the localized structure affects its collective rotation [23] and, therefore, determines the value of the angular velocity. As can be seen from Fig. 1, the latter can be positive, negative, or 0. Figure 3 shows the dependences of the angular velocity ω on the modulational depth p (for $k = 1$, $l = 1$) which were obtained from variational and exact numerical solutions of Eq. (7). A very good agreement is evident.

V. STABILITY AND GENERATION OF AZIMUTHAL CLUSTERS

Numerical stability analysis shows that most of the azimuthal clusters are unstable. However, both nonrotating ($\omega = 0$) and rotating two-peak single-charge vortices (azimuthons) $\langle -1, 1 \rangle$ have a large stability region in the parameter space (see Fig. 4). Such stable states can be found in other physical systems, for example, in nematic liquid crystals, where they were recently observed experimentally [41]. Other types of clusters can survive (provided the norm, \mathcal{N} , is not too large) over long times, comparable to the lifetime of the condensate (i.e., several seconds). Examples of the stable evolution of five-peak states are shown in Fig. 5.

The longevity of azimuthal clusters in certain parameter regions (i.e., for a certain normalized number of atoms \mathcal{N}

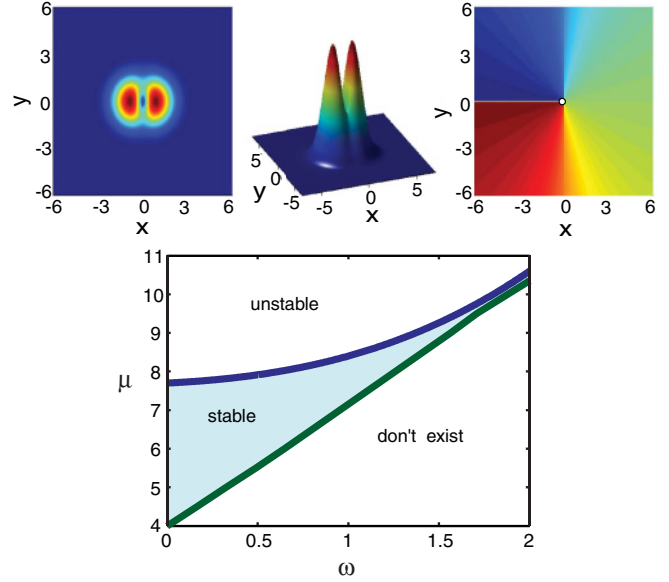


FIG. 4. (Color online) Top: Amplitude, $|\Phi|$, and phase structure of the two-peak azimuthon $\langle -1, 1 \rangle$ from the existence domains in Fig. (1) bordered by curve 1 ($\mu = 5$, $\omega = 0.2$). The phase changes from 0 (blue) to 2π (red); the vortex position is shown by the circle. Bottom: Stability region for the $\langle -1, 1 \rangle$ azimuthon for $\omega > 0$. For $\omega < 0$, the corresponding stability region is a mirror image of the one shown here.

and angular velocity ω) enables us to suggest a scheme for their dynamical excitation via phase imprinting [42]. More specifically, we employ a phase imprinting scheme which is similar to that used for excitation of azimuthons in optical experiments [26] and mimics the staircase-like azimuthal phase winding structure. In our numerical simulations, we start with a variationally determined Gaussian density distribution, which is close to the ground-state wave function of a BEC with norm \mathcal{N} in the 2D harmonic trap. We take the initial

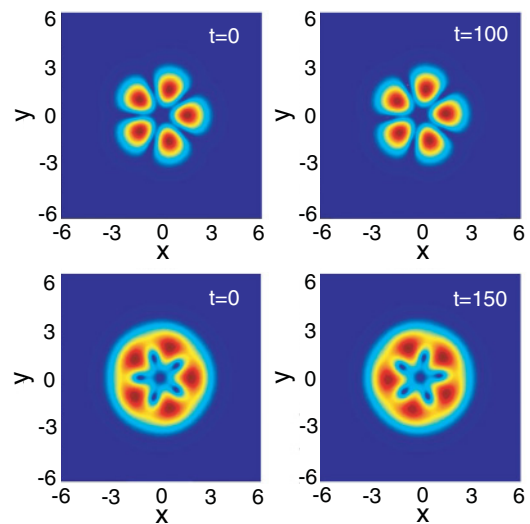


FIG. 5. (Color online) Initial amplitude structures and results of temporal evolution of a dynamically stable azimuthal cluster with $N = 5$. Top row: total charge $m = 3$, $\mu = 7$, $\omega = 0.4$. Bottom row: total charge $m = 4$, $\mu = 5.5$, $\omega = 1.19$. Evolution time, t , is measured in units of $2/\Omega_z$ (see text).

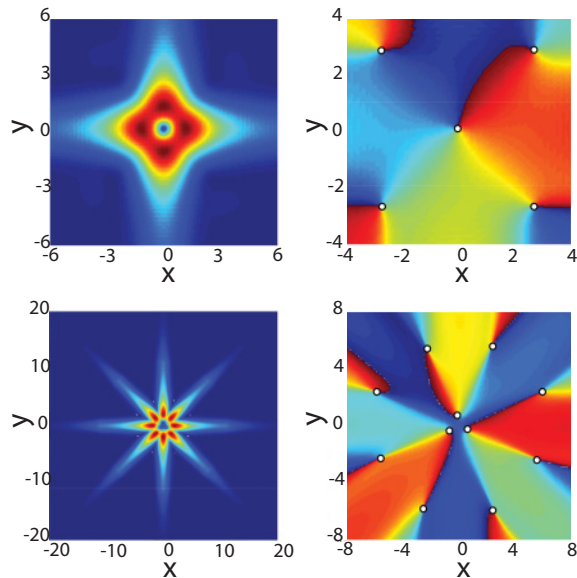


FIG. 6. (Color online) Dynamical generation of azimuthal vortex clusters after the evolution time $t = 0.8$, where time is measured in units of $2/\Omega_z$ (see text). Top row: a cluster with $N = 4$ and total charge $m = 3$; Bottom row: a cluster with $N = 8$ and total charge $m = 5$. The instantaneous amplitude $|\psi|$ of the BEC wave function (left) and the phase structure, $\arg(\psi)$, in the core area (right). The phase changes from 0 (blue) to 2π (red); vortex positions are marked by circles.

states with $\mathcal{N} \approx 50$. The actual number of atoms in the condensate is proportional to $\mathcal{N}(a_0/a_s)$ and, depending on the atomic species and trapping frequencies, can take values of the order of 10^5 – 10^6 . We then multiply the Gaussian wave function by a phase factor with stepwise phase dependence on the azimuthal angle: $\phi(\theta) = 2\pi m_c n_N / N$ for $2\pi n_N / N < \theta < 2\pi(n+1)/N$, where $n_N = 0 \dots N-1$. We fix the number of peaks N targeted by the excitation process and the central charge $m_c < 0$ such that $|m_c| \leq N/2$, thus the total phase winding is split into N segments. Indeed, the subsequent time evolution of the BEC cloud results in the formation of an azimuthal cluster with N peaks, central charge m_c , a total of $N+1$ singularities, and total charge (including N periphery singularities with the charge $+1$ each) $m = N + m_c$ ($m = N - |m_c|$). An example of the dynamically excited azimuthal cluster with $N = 4$ is shown in Fig. 6 (top row) for a short evolution time after excitation (for the trapping setup in [37] this time corresponds to ≈ 4 ms). In this case the total charge of the cluster is $m = 3$, the cluster displays the topological charge of the central singularity $m_c = -1$, and there are four singularities on the periphery with topological charge $+1$. In general, for longer evolution times, azimuthal vortex clusters display oscillatory, recurrent dynamics while preserving the singularity texture. In the case of a higher charge

of the central singularity, it can split into single-charge vortices. However, these vortices also form a robust regular pattern in the central area of the cluster which is preserved with time. An example of such a structure, an eight-lobe cluster with $m = 5$, is shown in the bottom row in Fig. 6. The charge of the central singularity is $m_c = -3$, and eight singularities on the periphery with topological charge $+1$ have been generated in the process of dynamical excitation. The central singularity has split into three vortices, forming a stable pattern at the core of the cluster.

The extremely robust excitation scheme numerically tested here would be quite involved experimentally [26], since it requires the transfer of a complex phase state from photons to atomic cloud. However, our proof-of-principle simulations clearly demonstrate one-to-one correspondence between the phase texture of the azimuthon and its density structure, which can be controlled in a deterministic fashion via phase imprinting. Other possible excitation schemes can be proposed. The experimental phase imprinting techniques achieved via angular momentum transfer from optical fields to atoms [43] can enable us to imprint an arbitrary total topological charge onto a condensate cloud using superposition of vortex states [44]. Likewise, a laser-illuminated mask can be used to impose a density modulation onto a 2D BEC cloud [12]. Therefore, experimental schemes of azimuthon excitation via simultaneous phase and density imprinting can, in principle, be investigated and tested. However, our preliminary results on this excitation method show that it suffers from interference-induced instabilities of the azimuthal vortex cluster [14], and although the targeted phase texture is reproduced, the amplitude structure of the azimuthal cluster is easily destroyed.

VI. CONCLUSIONS

The azimuthal vortex clusters in BECs that are described here represent a broad class of spatially localized stationary and rotating states containing multiple vortices. These stationary states exist in both rotating and nonrotating BEC clouds with repulsive interatomic interaction confined by a harmonic trap. The remarkable feature of these states is the one-to-one correspondence between phase texture and density modulation, which makes them analogous to other globally linked multivortex states, such as H clusters [45]. Finally, we have demonstrated numerically that the robust dynamics of these states may enable their dynamical excitation via phase imprinting by the transfer of a nontrivial angular momentum state from photons to atoms.

ACKNOWLEDGMENTS

This work was supported by the Australian Research Council (ARC). V.M.L. thanks the Nonlinear Physics Centre for hospitality during his stay at the Research School of Physics and Engineering, The Australian National University.

- [1] K. W. Madison, F. Chevy, W. Wohlleben, and J. Dalibard, *Phys. Rev. Lett.* **84**, 806 (2000).
 [2] B. P. Anderson, P. C. Haljan, C. E. Wieman, and E. A. Cornell, *Phys. Rev. Lett.* **85**, 2857 (2000).

- [3] P. Rosenbusch, V. Bretin, and J. Dalibard, *Phys. Rev. Lett.* **89**, 200403 (2002).
 [4] Y. Shin, M. Saba, M. Vengalattore, T. A. Pasquini, C. Sanner, A. E. Leanhardt, M. Prentiss, D. E. Pritchard, and W. Ketterle, *Phys. Rev. Lett.* **93**, 160406 (2004).

- [5] D. V. Freilich, D. M. Bianchi, A. M. Kaufman, T. K. Langin, and D. S. Hall, *Science* **329**, 1182 (2010).
- [6] T. W. Neely, E. C. Samson, A. S. Bradley, M. J. Davis, and B. P. Anderson, *Phys. Rev. Lett.* **104**, 160401 (2010)
- [7] M. Möttönen, S. M. M. Virtanen, T. Isoshima, and M. M. Salomaa, *Phys. Rev. A* **71**, 033626 (2005).
- [8] J. A. Seman, E. A. L. Henn, M. Haque, R. F. Shiozaki, E. R. F. Ramos, M. Caracanhas, P. Castilho, C. Castelo Branco, P. E. S. Tavares, F. J. Poveda-Cuevas, G. Roati, K. M. F. Magalhaes, and V. S. Bagnato, *Phys. Rev. A* **82**, 033616 (2010).
- [9] L.-C. Crasovan, V. Vekslershik, V. M. Pérez-García, J. P. Torres, D. Mihalache, and L. Torner, *Phys. Rev. A* **68**, 063609 (2003).
- [10] J. R. Abo-Shaeer, C. Raman, J. M. Vogels, and W. Ketterle, *Science* **292**, 476 (2001).
- [11] P. Engels, I. Coddington, P. C. Haljan, and E. A. Cornell, *Phys. Rev. Lett.* **89**, 100403 (2002).
- [12] D. R. Scherer, C. N. Weiler, T. W. Neely, and B. P. Anderson, *Phys. Rev. Lett.* **98**, 110402 (2007).
- [13] R. Carretero-González, B. P. Anderson, P. G. Kevrekidis, D. J. Frantzeskakis, and C. N. Weiler, *Phys. Rev. A* **77**, 033625 (2008).
- [14] G. Ruben, D. M. Paganin, and M. J. Morgan, *Phys. Rev. A* **78**, 013631 (2008).
- [15] J. R. Anglin and W. H. Zurek, *Phys. Rev. Lett.* **83**, 1707 (1999).
- [16] A. S. Bradley, C. W. Gardiner, and M. J. Davis, *Phys. Rev. A* **77**, 033616 (2008).
- [17] F. Dalfovo and S. Stringari, *Phys. Rev. A* **53**, 2477 (1996).
- [18] Y. Castin and R. Dum, *Eur. Phys. J. D* **7**, 399 (1999).
- [19] K. W. Madison, F. Chevy, V. Bretin, and J. Dalibard, *Phys. Rev. Lett.* **86**, 4443 (2001).
- [20] E. Hodby, G. Hechenblaikner, S. A. Hopkins, O. M. Maragó, and C. J. Foot, *Phys. Rev. Lett.* **88**, 010405 (2001).
- [21] V. M. Lashkin, *Phys. Rev. A* **77**, 025602 (2008); **78**, 033603 (2008).
- [22] V. M. Lashkin, E. A. Ostrovskaya, A. S. Desyatnikov, and Yu. S. Kivshar, *Phys. Rev. A* **80**, 013615 (2009).
- [23] A. S. Desyatnikov, A. A. Sukhorukov, and Yu. S. Kivshar, *Phys. Rev. Lett.* **95**, 203904 (2005).
- [24] S. Lopez-Aguayo, A. S. Desyatnikov, Yu. S. Kivshar, S. Skupin, W. Krolikowski, and O. Bang, *Opt. Lett.* **31**, 1100 (2006).
- [25] S. Lopez-Aguayo, A. S. Desyatnikov, and Yu. S. Kivshar, *Opt. Express* **14**, 7903 (2006).
- [26] A. Minovich, D. N. Neshev, A. S. Desyatnikov, W. Królikowski, and Yu. S. Kivshar, *Opt. Express* **17**, 23610 (2009).
- [27] J. Zheng and L. Dong, *J. Opt. Soc. Am. B* **28**, 780 (2011).
- [28] A. S. Desyatnikov and Yu. S. Kivshar, *Phys. Rev. Lett.* **88**, 053901 (2002).
- [29] D. Buccoliero, A. S. Desyatnikov, W. Krolikowski, and Yu. S. Kivshar, *Phys. Rev. Lett.* **98**, 053901 (2007).
- [30] Y. Zhang, S. Skupin, F. Maucher, A. Galestian Pour, K. Lu, and W. Królikowski, *Opt. Express* **18**, 27846 (2010).
- [31] E. A. Ostrovskaya, T. J. Alexander, and Yu. S. Kivshar, *Phys. Rev. A* **74**, 023605 (2006).
- [32] T. J. Alexander, A. S. Desyatnikov, and Yu. S. Kivshar, *Opt. Lett.* **32**, 1293 (2007).
- [33] B. Terhalle, T. Richter, A. S. Desyatnikov, D. N. Neshev, W. Krolikowski, F. Kaiser, C. Denz, and Yu. S. Kivshar, *Phys. Rev. Lett.* **101**, 013903 (2008).
- [34] D. Leykam and A. S. Desyatnikov, *Opt. Lett.* **36**, 4806 (2011).
- [35] G. Ruben, M. J. Morgan, and D. M. Paganin, *Phys. Rev. Lett.* **105**, 220402 (2010).
- [36] V. M. Pérez-García, H. Michinel, and H. Herrero, *Phys. Rev. A* **57**, 3837 (1998).
- [37] A. Görlitz, J. M. Vogels, A. E. Leanhardt, C. Raman, T. L. Gustavson, J. R. Abo-Shaeer, A. P. Chikkatur, S. Gupta, S. Inouye, T. Rosenband, and W. Ketterle, *Phys. Rev. Lett.* **87**, 130402 (2001).
- [38] D. Rychtarik, B. Engeser, H.-C. Nägerl, and R. Grimm, *Phys. Rev. Lett.* **92**, 173003 (2004).
- [39] F. Maucher, D. Buccoliero, S. Skupin, M. Grech, A. S. Desyatnikov, and W. Krolikowski, *Opt. Quantum Electron.* **41**, 337 (2009).
- [40] For example, the variational procedure for a three-peak azimuthal cluster with $k = 1$, $l = 2$, and $\mu = 5$, $\omega = 0.7$ yields $A = 0.99$, $a = 1.018$, $s = 0.26$. We took the variational solution as an initial guess, and after 32 iterations and smooth convergence, the norm of the residual fell below 10^{-9} .
- [41] Ya. V. Izdebskaya, A. S. Desyatnikov, G. Assanto, and Yu. S. Kivshar, *Opt. Express* **19**, 21457 (2011).
- [42] L. Dobrek, M. Gajda, M. Lewenstein, K. Sengstock, G. Birkl, and W. Ertmer, *Phys. Rev. A* **60**, R3381 (1999).
- [43] M. F. Andersen, C. Ryu, P. Cladé, V. Natarajan, A. Vaziri, K. Helmerson, and W. D. Phillips, *Phys. Rev. Lett.* **97**, 170406 (2006).
- [44] K. T. Kapale and J. P. Dowling, *Phys. Rev. Lett.* **95**, 173601 (2005).
- [45] L.-C. Crasovan, G. Molina-Terriza, J. P. Torres, L. Torner, V. M. Pérez-García, and D. Mihalache, *Phys. Rev. E* **66**, 036612 (2002).